

PAPER • OPEN ACCESS

Research on Fault Diagnosis of Analog Circuit Based on Volterra Theory and Higher-Order Spectrum Analysis

To cite this article: Kun Wang *et al* 2020 *IOP Conf. Ser.: Mater. Sci. Eng.* **782** 032096

View the [article online](#) for updates and enhancements.

You may also like

- [An incipient fault diagnosis method based on Att-GCN for analogue circuits](#)
Jingli Yang, Ye Li and Tianyu Gao
- [POWERFUL ROTATING DISK WINDS FROM STELLAR-MASS BLACK HOLES](#)
J. M. Miller, A. C. Fabian, J. Kaastra et al.
- [Review of recent trends in flexible metal oxide thin-film transistors for analog applications](#)
Giuseppe Cantarella, Júlio Costa, Tilo Meister et al.



ECS
The
Electrochemical
Society
Advancing solid state &
electrochemical science & technology

DISCOVER
how sustainability
intersects with
electrochemistry & solid
state science research

Research on Fault Diagnosis of Analog Circuit Based on Volterra Theory and Higher-Order Spectrum Analysis

KunWang*, YuanGuan^a, Dameng Li^b, Xiuquan Li^c and Jinfeng Guan^d

Beijing Smartchip Microelectronics Technology Co., Ltd., Beijing, China

*Corresponding author e-mail: wkshanghj@163.com, ^aguanyuan@sgitg.sgcc.com.cn, ^blidameng@sgitg.sgcc.com.cn, ^clixuquan@sgitg.sgcc.com.cn, ^dguanjinffeng@sgitg.sgcc.com.cn

Abstract. To diagnose fault of nonlinear components in analog circuits, a method of fault diagnosis based on Volterra series theory, high-order spectrum and kernel assurance criterion (KAC) analysis was proposed. Firstly, input and output signals of the analog circuit were used to identify a Volterra model. Secondly, the kernel function was solved by the improved multi-pulse excitation method. The high-order spectrum and its slice method were used to qualitatively characterize the kernel function. Finally, the concept of KAC indicator was introduced to quantitatively compare the characteristics of soft faults in the analog circuit, and the fault degree information was extracted and diagnosed. Taking the Sallen-key filter circuit as the research object, the simulation of the method shows that the high-order spectrum and KAC index can be used to quantify the Volterra system with different fault levels, which can effectively distinguish analog circuit with different soft faults, and have certain practical significance.

1. Introduction

With the development of high-tech products such as communication and space equipment, the functions and performance of SOC chips are becoming more and more strict. Fault feature extraction and identification of chips have been hot topics for recent years. Due to the different nature and the higher nonlinearity of the analog circuit in the chip circuit test, it is difficult to diagnose fault and identify parameter. It is of great significance to perform analog circuit fault diagnosis and parameter identification.

For the analog integrated circuit, due to the influence of the product process, the component parameters will be randomly offset from the standard value, and lead to different degrees of circuit performance changes. According to the degree of offset, the fault type can be classified into soft and hard fault [1]. Hard faults are caused by large defects in design or production such as open or short circuits problems, which cause the completely failure of circuit. The parameters of the component change is caused by soft fault such as manufacturing tolerances, temperature drift, etc. [2], and the circuit with such fault has good function but large performance deviation. Due to the small deviation of the performance parameters of the soft fault, it is difficult to extract the fault features and identify the parameters in the nonlinear analog circuit. Such problems are focus on scholars at home and abroad in recent years. M. Tadeusiewicz et al. have developed a neural-network based analog fault diagnostic



system for actual circuits, the collected data is preprocessed by wavelet decomposition, and take the actual circuit as an example to distinguish the faulty components [3]. VASAN S et al extract features for fault diagnosis through the continuous refinement of the scanning signal, and propose a nuclear method to solve the fault identification as a pattern recognition problem, and a case study is carried out to prove the effectiveness of the method through two kinds of analog filter circuit [4]. However, such methods are greatly affected by the nonlinearity of the analog circuit, and it is difficult to identify the soft fault of the analog integrated circuit stably. In recent years, many scholars have focused on the fault identification of nonlinear analog circuits. YANG Chen-lin et al. proposed a new modeling method that can be applied to linear and nonlinear circuits, and verified by simulation and experiment. [5] Han Haitao et al. [6] proposed a new method for fault mode discrimination using kernel principal component analysis (KPCA) and multi-class support vector machine (MSVM). The fault simulation is performed by the Sallen-Key band-pass filter. It proves that this method has the high accuracy of analog circuit parameter type fault identification. The above research content has achieved certain results in the fault diagnosis of nonlinear analog circuits, but there are still a series of problems such as complex algorithms and poor convergence. Aiming at such problems, this paper proposes an improved Volterra series modeling [7] and KAC index in nonlinear analog circuits as evaluation indicators, and to identify the soft faults of nonlinear analog circuits, and verify the correctness and superiority of the method through simulation experiments.

2. Proposed method

The nonlinear circuit fault simulation is carried out based on MATLAB and PSPICE,. The Volterra series model is established by using the input and output data of this circuit. The improved multi-pulse excitation method is used to solve the Volterra kernel function, and is identified by the generalized frequency response function (GFRF), and the different degrees of failure on the system is visually represented by the high-order spectrum. For the shortcomings of the lack of quantitative results of the high-order spectrum, the KAC index is used to quantitatively describe the different fault levels of the Volterra model. and has achieved good results in the identification and diagnosis of nonlinear analog circuits with different degrees of failure. The fault feature extraction method based on Volterra series and high-order impulse response function confidence criteria is as follows:

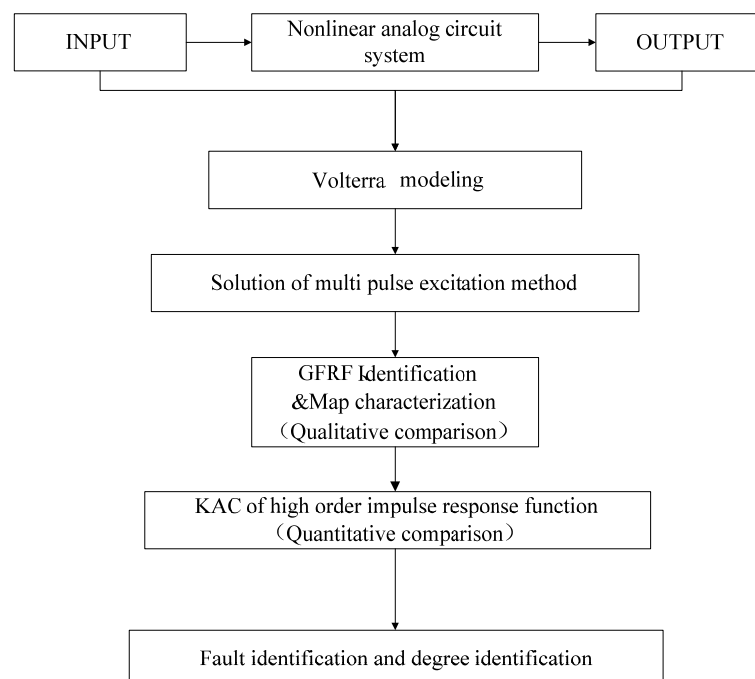


Figure 1. Volterra series and higher order spectrum and KAC analysis

3. Volterra series theory

3.1. Basic concept

Volterra series theory was first proposed from the mathematical point, mainly applied to the solution of mathematically complex calculus equations [8]. It can be used to describe nonlinear systems by modeling, and is widely used in nonlinear modeling and analysis in the fields of electronics and machinery [9]. The core is the representation of system output through the multidimensional convolution of the kernel function and the input signal of the system. The basic definition is:

$$y(t) = h_0(t) + \sum_{k=1}^{\infty} \int_0^{\infty} \cdots \int_0^{\infty} h_k(\tau_1, \tau_2, \dots, \tau_k) \prod_{i=1}^k \mu(t - \tau_i) d\tau_i \quad (1)$$

The input and output of the system separately are $\mu(\tau)$ and $y(t)$, the order $h_k(\tau_1, \tau_2, \dots, \tau_k)$ is the Volterra kernel function for this system. As can be seen from equation (1), for a linear system, its Volterra series model can be expressed as:

$$y(t) = \int_{-\infty}^{\infty} h(t - \tau) \mu(\tau) d\tau \quad (2)$$

$\mu(\tau)$ and $y(t)$ represent the system input and output, and $h(\tau)$ is equivalent to the impulse response function of the linear system. Therefore, Volterra series is the mapping and generalization of the transfer function in nonlinear systems. Its physical meaning is consistent with the system transfer function, which represents the fundamental characteristics of the system, and is independent of system input and output. Based on this characteristic, the nonlinear system can be characterized by Volterra series, which can fully describe the nonlinear system characteristics and avoid the influence of system nonlinearity and discreteness.

It can be seen from Equation 2 that it represents the system characteristics of a linear system. Similarly, the mapping to a nonlinear system, $h(\tau), h(\tau_1, \tau_2), h(\tau_1, \tau_2, \tau_3)$ represents a system characteristic of a nonlinear system. Therefore, for a nonlinear system, determine its system characteristics are fundamentally determining the Volterra kernel function.

Considering the discreteness of the nonlinear system, in order to better describe its characteristics, it can be discretized as the following form that compared to a linear system:

$$y(n) = y_0 + \sum_{n=1}^{\infty} \sum_{i_1=0}^{\infty} \cdots \sum_{i_k=0}^{\infty} h_k(i_1, i_2, \dots, i_k) \prod_{k=1}^{\infty} u(n - i_k) \quad (3)$$

For the solution of this discrete form, it is necessary to determine the specific value of n and m in practice, so the variant can be obtained:

$$y(n) = \sum_{n=1}^N \sum_{m_1=0}^{M-1} \cdots \sum_{m_n=0}^{M-1} h_0(m_1, m_2, \dots, m_k) \prod_{i=1}^n u(n - m_i) + e(k) \quad (4)$$

Where N is the maximum order of the identified system and M is the system memory length, and $e(k)$ is the truncation error generated from the nonlinear system after its truncated form is determined. Therefore, the solution to the discrete form can be realized in the case of system convergence. As long as the truncated form of the system is determined, the system kernel function can be determined through a series of algorithms, thereby fundamentally describing the system characteristics.

Similarly, to describe the system characteristics, it reflects not only from the time domain, but need to be transformed into the frequency domain by multi-dimensional fourier transform, and to analyze the system characteristics further. The frequency domain expression is:

$$Y(\omega) = \sum_{n=1}^{\infty} Y_n(\omega)$$

$$Y_n(\omega) = \frac{1}{(2\pi)^{n-1}} \int_{-\infty}^{\infty} \int_{-\infty}^{\infty} \cdots \int_{-\infty}^{\infty} H_n(\omega - \omega_2 - \cdots - \omega_n, \omega_2, \dots, \omega_n) \times$$

$$U(\omega - \omega_2 - \cdots - \omega_n, \omega_2, \dots, \omega_n) U(\omega_2) \cdots U(\omega_n) d\omega_2 \cdots d\omega_n \quad (5)$$

Among them, $U(\omega)$ and $Y_n(\omega)$ are obtained by fourier transform from $u(t)$ and $y(t)$. Similarly, $H_n(\omega, \omega_2, \dots, \omega_n)$ through the multi-dimensional fourier transform of the time-domain kernel of the n order Volterra series is called the n order GFRF of the nonlinear system or the frequency domain kernel.

$$H_n(\omega_1, \omega_2, \dots, \omega_n) = \int_{-\infty}^{\infty} \cdots \int_{-\infty}^{\infty} h_n(\tau_1, \tau_2, \dots, \tau_n)$$

$$e^{-j(\omega_1\tau_1 + \omega_2\tau_2 + \cdots + \omega_n\tau_n)} d\tau_1 d\tau_2 \cdots d\tau_n \quad (6)$$

Since the GFRF of Volterra series is generalized on the basis of the linear system frequency response function, its essence is the same, so the GFRF of the nonlinear system is a non-parametric model, which can also represent the frequency domain characteristics of many systems, and are visually described when performing nonlinear analysis identification.

3.2. Multi-pulse excitation method

Suppose there is a nonlinear system that can be described by a third-order Volterra kernel function as follows:

$$y(t) = \int_0^t h_1(t - \tau_1) u(\tau_1) d\tau_1 + \int_0^t \int_0^t h_2(t - \tau_1, t - \tau_2) u(\tau_1) u(\tau_2) d\tau_1 d\tau_2 \quad (7)$$

Taking a pulse excitation as input, according to the convolution theorem, the system output is expressed as follows:

$$\mu_0(t) = a_\delta \delta(t) \rightarrow y_0(t)$$

$$y_0(t) = a_\delta h_1(t) \quad (8)$$

After transposition, the first-order kernel function is obtained as:

$$h_1(t) = \frac{y_0(t)}{a_\delta} \quad (9)$$

Similarly, two different amplitude pulse excitations are input to the system, and the output is expressed as follows:

$$\begin{cases} \mu_0(t) = a_\delta \delta(t) \rightarrow y_0(t) \\ y_0(t) = a_\delta h_1(t) + a_\delta^2 h_2(t, t) \end{cases} \quad (10)$$

$$\begin{cases} \mu_0(t) = 2a_\delta \delta(t) \rightarrow y_1(t) \\ y_1(t) = 2a_\delta h_1(t) + 4a_\delta^2 h_2(t, t) \end{cases} \quad (11)$$

Converting to a matrix can be expressed as:

$$\begin{bmatrix} a_\delta & a_\delta^2 \\ 2a_\delta & 4a_\delta^2 \end{bmatrix} \begin{bmatrix} h_1(t) \\ h_2(t, t) \end{bmatrix} = \begin{bmatrix} y_0(t) \\ y_1(t) \end{bmatrix} \quad (12)$$

Therefore, the second-order kernel function of the system is solved as follows:

$$\begin{cases} h_1(t) = \frac{4y_0(t) - y_1(t)}{2a_\delta} \\ h_2(t) = \frac{y_1(t) - 2y_0(t)}{2a_\delta^2} \end{cases} \quad (13)$$

Similarly, the solution of the third-order kernel function is:

$$\begin{cases} h_1(\tau_1) = \frac{18y_0(t) - 9y_1(t) + 2y_2(t)}{6a_\delta} \\ h_2(\tau_1, \tau_2) = \frac{4y_1(t) - 5y_0(t) - y_2(t)}{2a_\delta^2} \\ h_3(\tau_1, \tau_2, \tau_3) = \frac{3y_0(t) + y_2(t) - 3y_1(t)}{6a_\delta^3} \end{cases} \quad (14)$$

For systems represented by third-order or higher kernel functions, more different magnitudes of pulse excitation can be used as inputs to solve different order Volterra kernel functions, considering that as the order increases, the higher data dimension is generated, the more difficult the calculation is, due to the impact of this dimension disaster, it is more suitable to solve the kernel function mainly within the fourth order.

3.3. Simulation

Supposing there is a nonlinear system whose expression is as follows:

$$y_t = \frac{e^{-3v_t^2}}{e^{-v_t} + 1} \quad (15)$$

$$v_t = 2.1\mu_t + 1.3\mu_{t-1} + 0.6\mu_{t-2}$$

Performing a third-order Taylor expansion on the system and substituting v_t into it:

$$y_t = 0.5 - 2.75(2.1\mu_t + 1.3\mu_{t-1} + 0.6\mu_{t-2}) + 7.5(2.1\mu_t + 1.3\mu_{t-1} + 0.6\mu_{t-2})^2 + O(t_i^3) \quad (16)$$

The original second-order kernel function of the system can be obtained by the above formula:

$$\mathbf{h}_1 = -[5.775 \quad 3.575 \quad 1.65]$$

$$\mathbf{h}_2 = \begin{bmatrix} 33.075 & 20.475 & 9.45 \\ 20.475 & 12.675 & 5.85 \\ 9.45 & 5.85 & 2.7 \end{bmatrix} \quad (17)$$

According to the Volterra series theory, a pulse signal $\delta(t), \delta(t-T)$ with a certain delay is input to the system. The system output is recorded as y_1, y_2 . The estimated value of the system kernel function can be calculated by using Equation 12 as follows:

$$\mathbf{h}_1 = -[5.7746 \quad 3.573 \quad 1.6486]$$

$$\mathbf{h}_2 = \begin{bmatrix} 33.0728 & 20.453 & 9.4296 \\ 20.453 & 12.5625 & 5.7794 \\ 9.4296 & 5.7794 & 2.6496 \end{bmatrix} \quad (18)$$

In order to display the approximation more intuitively between the system kernel function and the Volterra kernel function calculated by the multi-pulse excitation method, the GFRF is obtained by using the discrete form of equation (4), thereby making the system first and second order amplitude-frequency and phase-frequency response curves, and intuitively illustrating that the Volterra kernel function solved by this method can best characterize the fundamental characteristics of nonlinear systems.

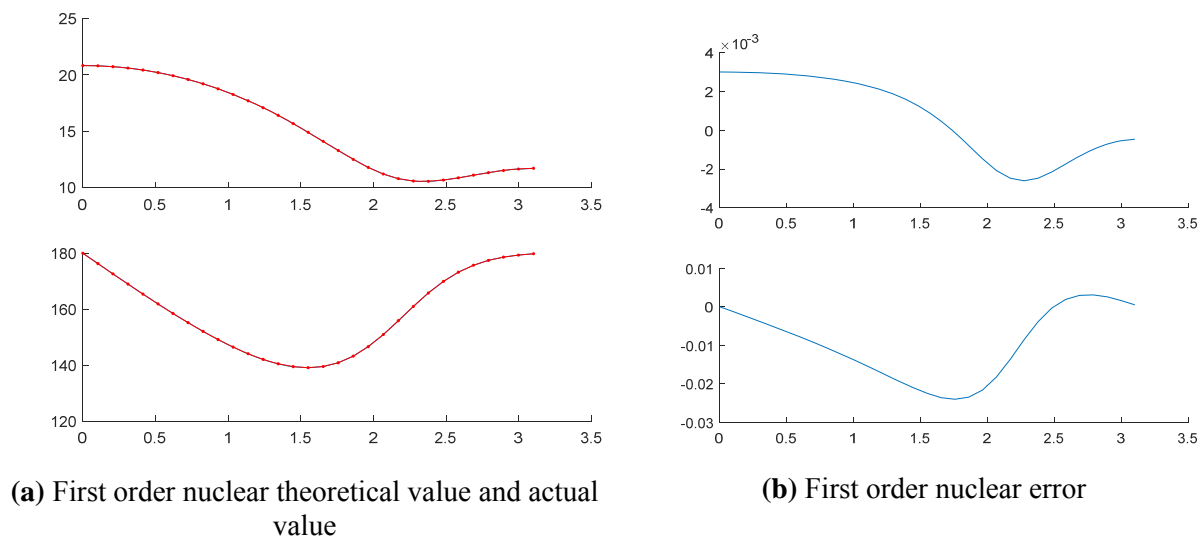


Figure 2 First-order kernel function identification

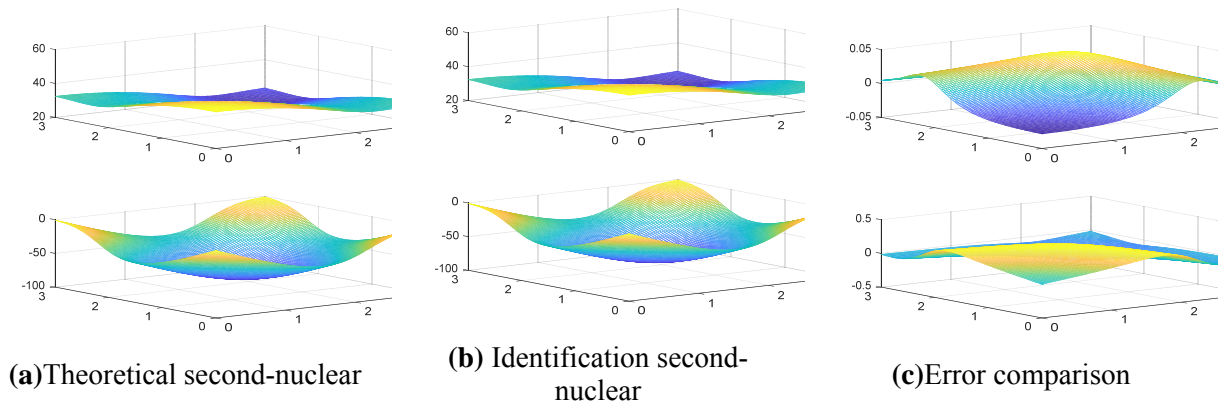


Figure 3 Second-order kernel function identification

Comparing Figure 2 and Figure 3, for the first-order kernel function, the maximum absolute error of amplitude and phase is 0.003dB and 0.025°, respectively, while the maximum absolute error of amplitude and phase of the second-order kernel function is 0.04 dB and 0.5°. The pulse excitation method solves the Volterra kernel function of the system, which can better identify the nonlinear system and characterize the system fundamentally.

4. High-order spectrum analysis

In practical applications, because of the influence of the external environment, it is difficult to eliminate the influence of external factors, that the GFRF of Volterra kernel function is used to represent and compare the system characteristics. And because the frequency response graph is a three-dimensional map, that quantitatively extract and compare the effective information difficultly.. In this paper, we can suppress the influence of Gaussian noise by using high-order spectrum, extract the features of Volterra kernel function with different fault degrees in the analog circuit, and perform diagonal slice processing on the bi-spectrum and tri-spectrum, finally, we compared and analyzed its fault characteristics. The characteristics are visually expressed, based on the frequency response function mode confidence criteria, mapped to the relevant indicators of the Volterra kernel function, which can be used to determine a fixed value to quantitatively describe the degree of faults generated in the analog circuit.

4.1. Bi-spectrum and Tri-Spectrum

The fourier transform of the autocorrelation function of a zero-mean continuous stationary random signal is defined as its power spectral density, and its autocorrelation function is absolutely reconcilable. Similarly, if the high-order cumulant $c_{kx}(\tau_1, \dots, \tau_{k-1})$ is absolutely reconcilable, then the k-order cumulant spectrum is defined as a $(k-1)$ dimensional discrete fourier transform of the k-order cumulant, which has the following definition:

$$S_{kx}(\omega_1, \dots, \omega_{k-1}) = \sum_{\tau_1=-\infty}^{\infty} \dots \sum_{\tau_{k-1}=-\infty}^{\infty} c_{kx}(\tau_1, \dots, \tau_{k-1}) e^{-j(\omega_1\tau_1 + \dots + \omega_{k-1}\tau_{k-1})} \quad (19)$$

In general, the high-order accumulation is often referred to high-order spectrum, also called multi-spectral [10]. In particular, the third-order spectrum $S_{3x}(\omega_1, \omega_2)$ is called bi-spectrum, and the fourth-order spectrum $S_{4x}(\omega_1, \omega_2, \omega_3)$ is called tri-spectrum. It is customary to use $B_x(\omega_1, \omega_2)$ to represent bispectrum and to use $T_x(\omega_1, \omega_2, \omega_3)$ to represent tri-spectrum. Using the Volterra kernel function

$h_k(\tau_1, \dots, \tau_k)$ obtained above as the nonlinear system kernel function, the conversion to the frequency domain can be obtained as a bi-spectrum representation formula:

$$B(\omega_1, \omega_2) = \gamma_{a,3} H(\omega_1) H(\omega_2) H^*(\omega_1 + \omega_2) \quad (20)$$

$$|B(\omega_1, \omega_2)| = \frac{|\gamma_{a,3}|}{\left| 1 + \sum_{i=1}^p \beta_i e^{-ji(\omega_1 + \omega_2)} \right| \left| \prod_{k=1}^2 \left| 1 + \sum_{i=1}^p \beta_i e^{-ji\omega_k} \right| \right|}$$

The expression of the tri-spectrum is:

$$T(\omega_1, \omega_2, \omega_3) = \gamma_{a,4} H(\omega_1) H(\omega_2) H(\omega_3) H^*(\omega_1 + \omega_2 + \omega_3) \quad (21)$$

$$|T(\omega_1, \omega_2, \omega_3)| = \frac{|\gamma_{a,4}|}{\left| 1 + \sum_{i=1}^p \gamma_i e^{-ji(\omega_1 + \omega_2 + \omega_3)} \right| \left| \prod_{k=1}^3 \left| 1 + \sum_{i=1}^p \gamma_i e^{-ji\omega_k} \right| \right|}$$

4.2. Slice spectrum

4.2.1. Three-spectrum two-dimensional slice spectrum. In practical applications, the tri-spectrum characterizes the phase coupling between three frequencies, which is composed of three frequencies and amplitudes. It is spatially a four-dimensional representation by using a movable ball in space generally, and the size of the sphere represents the three-spectrum amplitude of a certain point. As shown below:

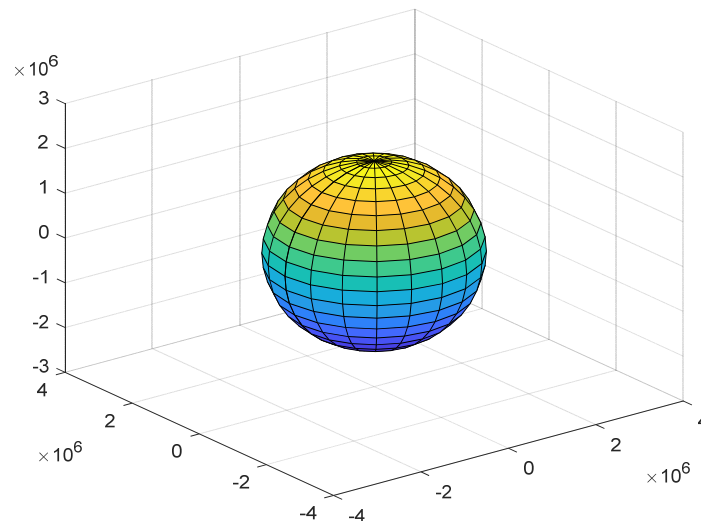


Figure 4 Tri-spectrum diagram

In order to display the tri-spectrum better in three-dimensional space, the frequency of $T(\omega_1, \omega_2, \omega_3)$ that any one of the formulas (16) is taken as the value, in general, $\omega=C=0$, the tri-spectrum can be

reduced to bi-spectrum, which is called the tri-spectrum's two-dimensional slice spectrum [11], its expression can be represented as follows:

$$T(\omega_1, \omega_2, C) = \gamma_{a,3} H(\omega_1) H(\omega_2) H(C) H^*(\omega_1 + \omega_2 + C) \quad (22)$$

The normalized magnitude expression for a tri-spectrum two -dimensional slice is:

$$|T(\omega_1, \omega_2, C)| = \frac{K}{\left| 1 + \sum_{i=1}^p \gamma_i e^{-ji(\omega_1 + \omega_2 + C)} \right| \prod_{k=1}^2 \left| 1 + \sum_{i=1}^p \gamma_i e^{-ji\omega_k} \right| \left| 1 + \sum_{i=1}^p \gamma_i e^{-jiC} \right|} \quad (23)$$

4.2.2. Diagonal slices of bi-spectrum and tri-spectrum. In order to make the two-dimensional slice spectrum and bispectrum display more intuitively, diagonally slice the bi-spectrum and tri-spectrum in the case of two-dimensional slicing, and express the tri-spectrum and bi-spectrum on the two-dimensional plane. There is an intuitive contrast between the bi-spectrum and tri-spectrum characterization phase coupling degrees.

In the bispectral expression (16), $\omega = \omega_1 = \omega_2$, the same as $B(\omega, \omega) = \gamma_{a,3} H(\omega)^2 H^*(2\omega)$, the magnitude of the normalized diagonal slice is:

$$|B(\omega, \omega)| = \frac{|S|}{\left| 1 + \sum_{i=1}^p \beta_i e^{-2ji\omega} \right| \left| 1 + \sum_{i=1}^p \beta_i e^{-ji\omega} \right|^2} \quad (24)$$

Similarly, in the three-dimensional slice expression of the tri-spectrum, the diagonal slice can be expressed as:

$$T(\omega, \omega, C) = \gamma_{a,3} H(\omega)^2 H(C) H^*(2\omega + C) \quad (25)$$

Its normalized magnitude is:

$$|T(\omega, \omega, C)| = \frac{K}{\left| 1 + \sum_{i=1}^p \gamma_i e^{-ji(2\omega + C)} \right| \left| 1 + \sum_{i=1}^p \gamma_i e^{-ji\omega} \right|^2 \left| 1 + \sum_{i=1}^p \gamma_i e^{-jiC} \right|} \quad (26)$$

4.3. Higher Order Impulse Response Function Confidence Criterion (KAC)

In mathematical definition, the SAC index at point k is defined as follows between the vector H_{pk} in the frequency response function (displacement, velocity or acceleration) of point P and the vector H_{qk} as the same:

$$SAC = \frac{\left(H_{pk}^T H_{qk} \right)^2}{\left(H_{pk}^T H_{pk} \right) \left(H_{qk}^T H_{qk} \right)} \quad (27)$$

Similarly, to the Volterra kernel function nonlinear system, this Volterra kernel function index can be defined as Kernel Assurance Criterion (KAC) [12], which is expressed as follows:

$$KAC_n = \frac{\left(\left| \sum_{\tau_1, \tau_2, \dots, \tau_n=0}^N h_n^u(\tau_1, \tau_2, \dots, \tau_n) h_n^c(\tau_1, \tau_2, \dots, \tau_n) \right|^2 \right)}{\left(\sum_{\tau_1, \tau_2, \dots, \tau_n=0}^N h_n^u(\tau_1, \tau_2, \dots, \tau_n) h_n^u(\tau_1, \tau_2, \dots, \tau_n) \right) \left(\sum_{\tau_1, \tau_2, \dots, \tau_n=0}^N h_n^c(\tau_1, \tau_2, \dots, \tau_n) h_n^c(\tau_1, \tau_2, \dots, \tau_n) \right)} \quad (28)$$

Where, $h_n^u(\tau_1, \tau_2, \dots, \tau_n)$ and $h_n^c(\tau_1, \tau_2, \dots, \tau_n)$ respectively represent the n-order Volterra kernel function of the system in the normal state and the fault state. According to equation (28), the second-order Volterra kernel function index of the system can be expressed as:

$$KAC_2 = \frac{\left(\left| \sum_{\tau_1, \tau_2=0}^N h_2^u(\tau_1, \tau_2) h_2^c(\tau_1, \tau_2) \right|^2 \right)}{\left(\sum_{\tau_1, \tau_2=0}^N h_2^u(\tau_1, \tau_2) h_2^u(\tau_1, \tau_2) \right) \left(\sum_{\tau_1, \tau_2=0}^N h_2^c(\tau_1, \tau_2) h_2^c(\tau_1, \tau_2) \right)} \quad (29)$$

Similarly, the third-order Volterra kernel function index of the system can be expressed as:

$$KAC_3 = \frac{\left(\left| \sum_{\tau_1, \tau_2, \tau_3=0}^N h_3^u(\tau_1, \tau_2, \tau_3) h_3^c(\tau_1, \tau_2, \tau_3) \right|^2 \right)}{\left(\sum_{\tau_1, \tau_2, \tau_3=0}^N h_3^u(\tau_1, \tau_2, \tau_3) h_3^u(\tau_1, \tau_2, \tau_3) \right) \left(\sum_{\tau_1, \tau_2, \tau_3=0}^N h_3^c(\tau_1, \tau_2, \tau_3) h_3^c(\tau_1, \tau_2, \tau_3) \right)} \quad (30)$$

Similar to the frequency response function mode confidence criterion SAC , the value of the indicator KAC is between zero and one, if the value is closer to one, the system is normal; otherwise, if the value is closer to zero, the system fails, and with the degree of failure increasing, the value is closer to zero, which is used as a basis and indicator for quantitatively judging different degrees of failure in the analog circuit.

5. Simulation experiment verification

In this paper, Volterra series and high-order spectrum are introduced into the analysis of analog circuits with different degrees of failure, and the degree of fault is quantified by KAC . The differences between different analog circuits with different degrees of fault are compared, and can analyze actual circuit failures in a certain sense.

The Sallen-key bandpass filter circuit is selected for verification, and specific circuit is shown in Figure 4:

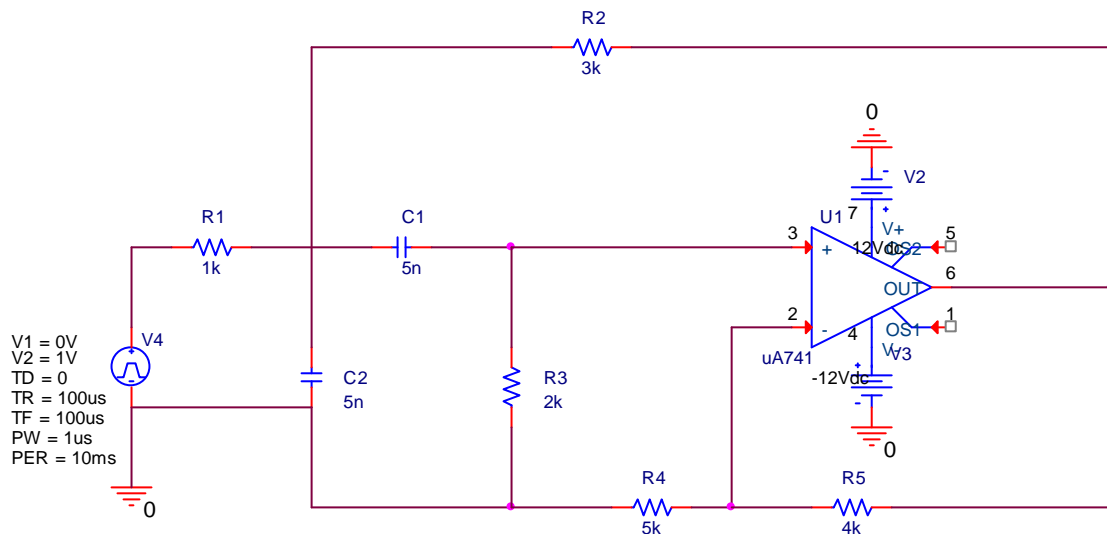
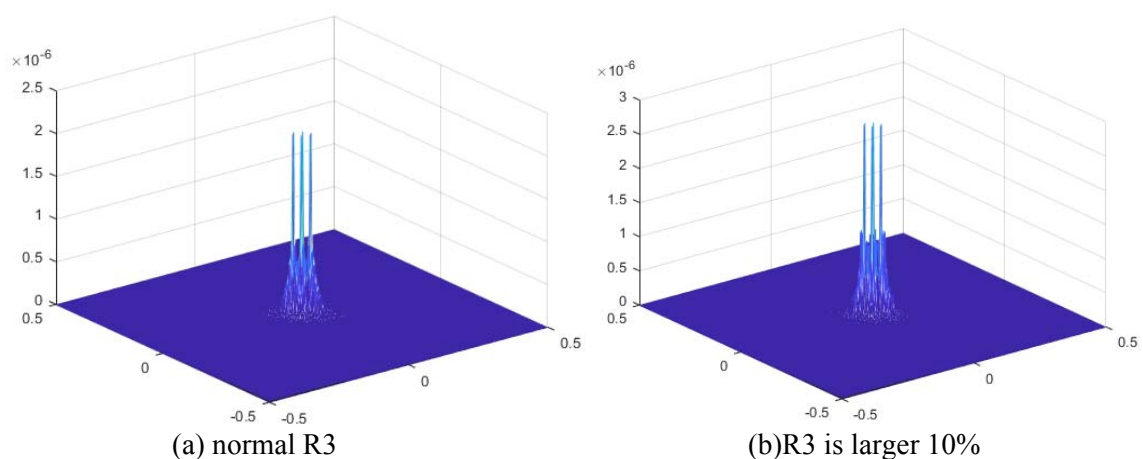
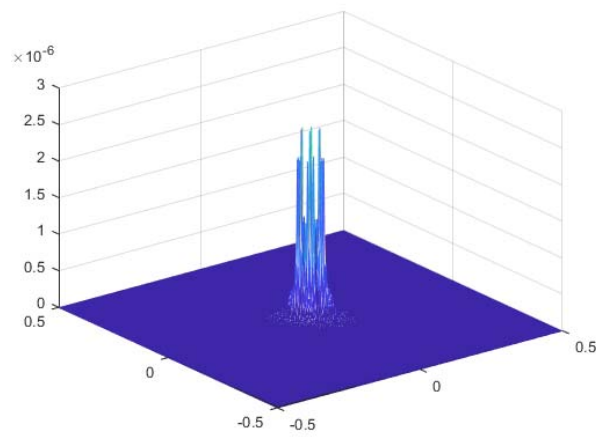


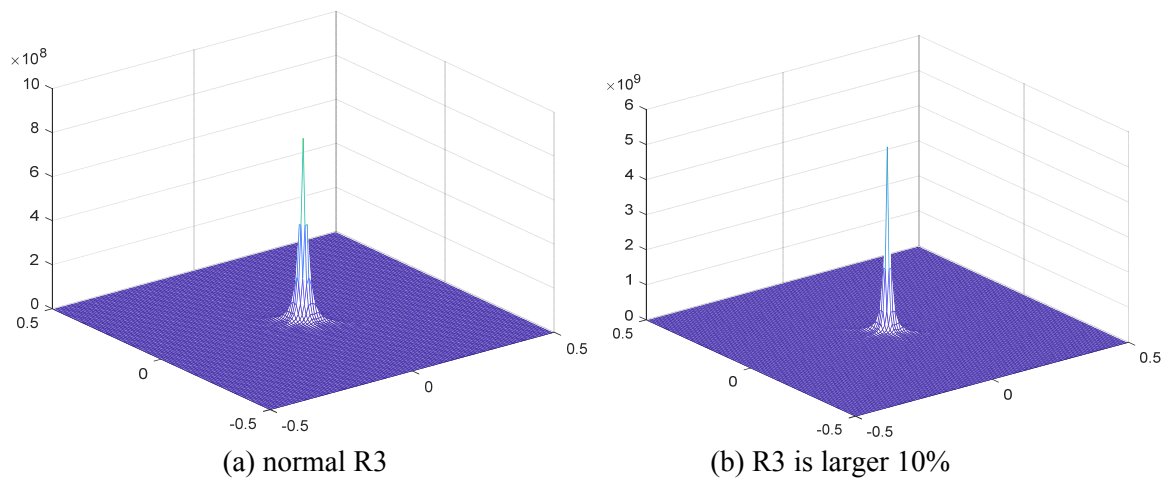
Figure 5 Sallen-key filter circuit

Taking this circuit as the research object, the influence of the resistance value changes on the system are studied. Generally, the resistance value is considered to be normal at $\pm 5\%$ of the standard value, and it is considered to be failed when the resistance value changes by more than $\pm 5\%$. Fault, when the device value exceeds $\pm 50\%$, it is considered damaged. In the PSPICE simulation circuit, R3 is selected as the analysis object, and the resistance is respectively set to normal, 10% floating and 20% floating. In the circuit, point 1 is the input node and point 4 is the output., according to the above multi-pulse excitation method, respectively to set the input excitation to $\sigma(t)$, $2\sigma(t)$, $3\sigma(t)$, and obtain the output data respectively as y_1 , y_2 , y_3 , finally, to process the output data through MATLAB to obtain the second-order and third-order kernel functions of the system, high-order spectrum and their slices are used to characterize the kernel function. The experimental software platform are PSPICE and MATLAB 2017a. The experimental results are shown in the following figures:



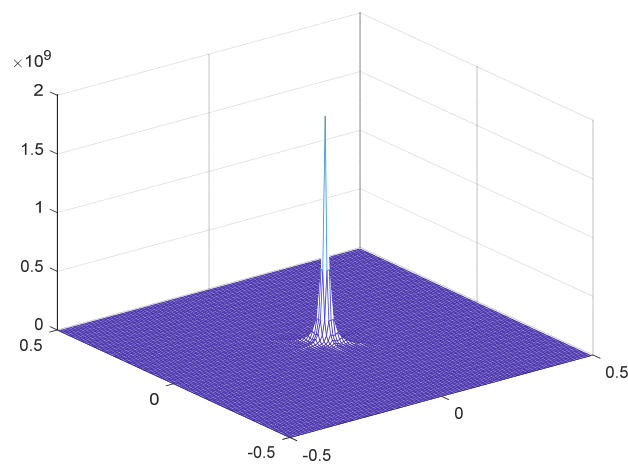


(c) R3 is larger 20%

Figure 6. Three-dimension graph of second-order kernel bi-spectrum

(a) normal R3

(b) R3 is larger 10%



(c) R3 is larger 20%

Figure 7. Second-dimension slice of the third-order kernel tri-spectrum

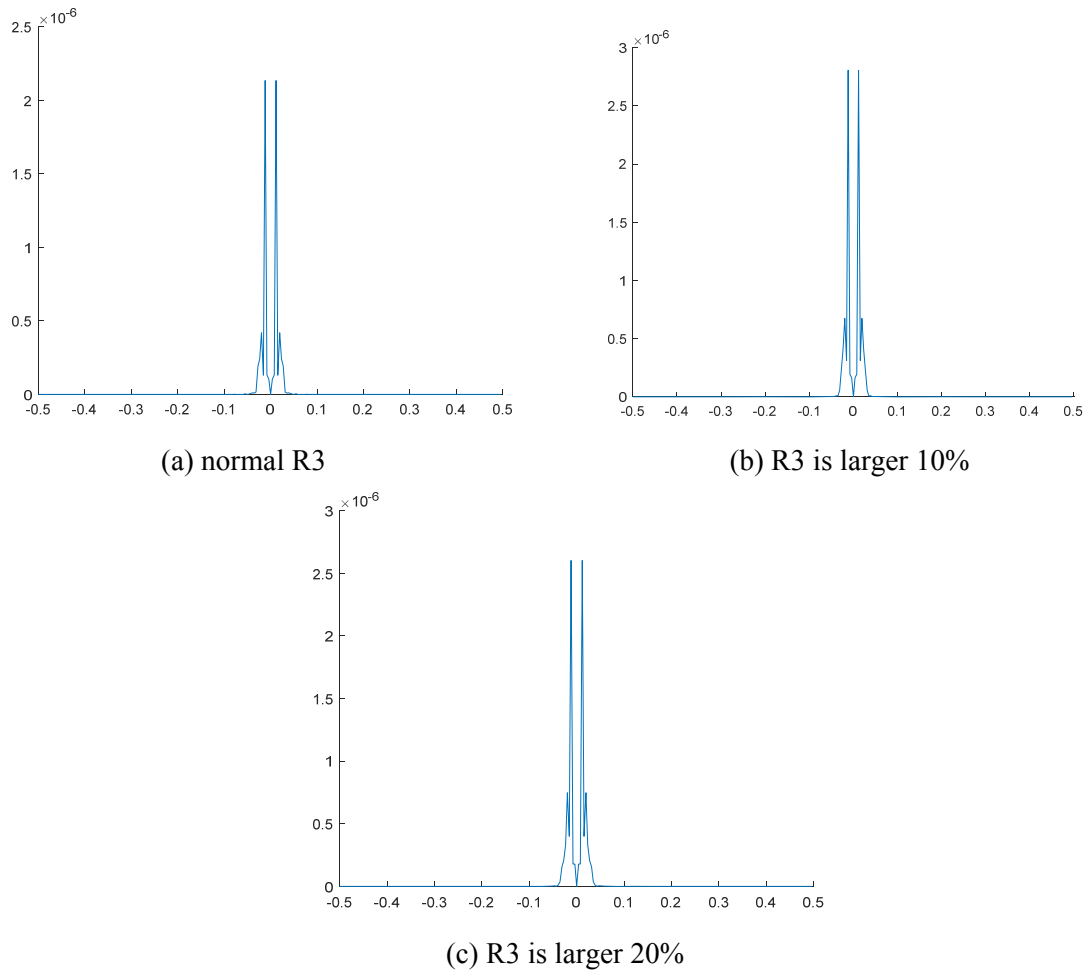
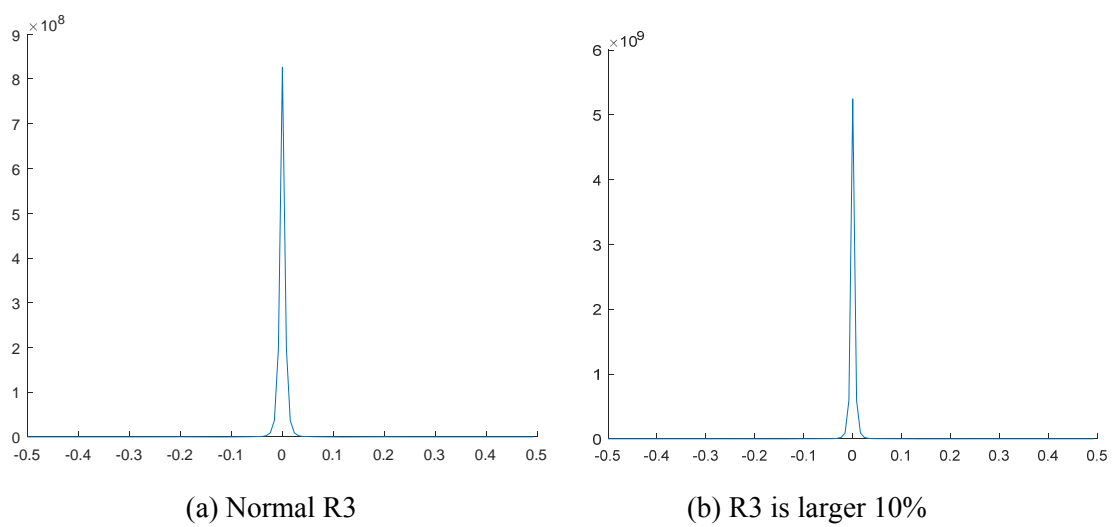
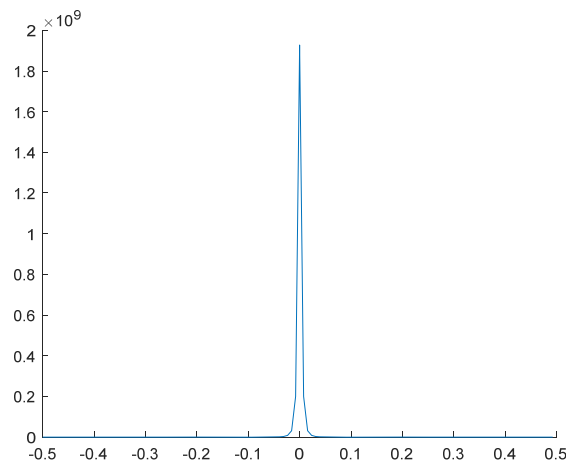


Figure 8. Second order kernel bi-spectrum slice





(c) R3 is larger 20%

Figure 9. Third order kernel tri-spectrum slice

Analysis of Fig. 6 and Fig. 7, the result shows that the high-order spectrum of the second-order and third-order kernel functions show a trend of increasing amplitude energy with the upward shift of the resistance value. It can be seen from the figure that the third-order nuclear energy represented by the two-dimensional slice is more concentrated, while the second-order nuclear energy represented by the bi-spectrum is more dispersed, indicating that for this system, the third-order kernel function characterizes the partially implied nonlinear features and can express the system characteristics in more detail.

In view of the fact that the three-dimensional bi-spectrum and the two-dimensional slice tri-spectrum are all three-dimensional forms, it is difficult to intuitively reflect the influence of the degree changes of the failure, so they are diagonally sliced separately, as shown in Fig. 8 and Fig. 9, the analysis result shows that as the resistance increases, the energy of the bi-spectrum and tri-spectrum slice shows an increase first and then a decrease, and the overall change is an increasing trend. Compared with the second-order nuclear function slice bispectrum, the energy distribution of the third-order nuclear slice tri-spectrum is more concentrated, the amplitude peak curve is reduced to one., and the magnitude of the energy can be extracted more intuitively, which can be quantified to some extent to describe the change in the degree of failure.

In summary, through the high-order spectrum and its slice spectrum, the second-order and third-order kernel functions can be characterized to some extent, but the change of the magnitude of the fault can only be compared from the change of the amplitude energy. As the degree of failure increases, the amplitude of the higher-order spectrum in the second-order and third-order kernel functions increases first and then decreases, and it is difficult to establish a one-to-one correspondence with the increasing degree of failure. Therefore, this paper introduces the KAC index to quantify the kernel functions of different orders, and uses R3, R4, and R5 as the analysis objects, and sets their resistance values to change by 10% each time, increasing to 50%, and decreasing to 20%. The following is expressed R3 \uparrow 10%, and R3 \downarrow 10%, the KAC indicators of the second-order and the third-order kernel are obtained, and the comparative analysis is shown in Table 1 below:

Table 1. Second- and third-order kernel KAC index with different degrees of failure

	R3			R4			R5		
	KAC ₁	KAC ₂	KAC ₃	KAC ₁	KAC ₂	KAC ₃	KAC ₁	KAC ₂	KAC ₃
↑10%	0.965	0.9399	0.9060	0.8491	0.7888	0.7698	0.9175	0.8696	0.8676
↑20%	0.9567	0.9122	0.8629	0.8312	0.7614	0.7546	0.8148	0.6972	0.6971
↑30%	0.8457	0.7047	0.6732	0.8108	0.6850	0.6724	0.775	0.6547	0.6563
↑40%	0.8266	0.6145	0.5846	0.7275	0.6179	0.6226	0.6514	0.4661	0.4435
↑50%	0.7701	0.4645	0.4233	0.5322	0.3285	0.3135	0.621	0.4181	0.4073
↓10%	0.8906	0.8668	0.8199	0.9628	0.9433	0.9382	0.8143	0.7910	0.7909
↓20%	0.662	0.7473	0.7047	0.8559	0.8008	0.8057	0.8711	0.6989	0.6975

The results in the above table show that as the degree of failure increases, the trend of KAC_2 and KAC_3 shows a gradual decline, and the rate of this decrease increases with the degree of failure, indicating that the greater the degree of failure is, even close to the device damaged, the more rapid decrease trend with the KAC index of each order kernel function is, and the degree changes of the fault can be quantified by the change of this index.

The changes of R3, R4, and R5 are analyzed separately, it can be seen that for R3 and R5, the KAC index is smaller when the resistance increases than that when the resistance decreases, but for the R4, the KAC index changes are bigger when the resistance value increases. than that when the resistance value decreases. It indicates that the KAC index is more sensitive to the increase of R3 and R5 than R4. Similarly, when the R4 resistance value decreases, the change in the function KAC indicator is more sensitive than R3 and R5.

Comparing the changes of KAC index of each order kernel function with the change of fault degree, it shows that the KAC index of the second-order and the third-order kernel function are more varied than the first-order kernel function, indicating that the related indicators of Volterra high-order kernel function that identified by the multi-pulse excitation method are more sensitive to the change of faults in this circuit. Therefore, this method can be used to perform system Volterra high-order kernel identification for analog circuit faults, and to compare the magnitude changes of different fault levels.

6. Conclusion

In this paper, a method based on Volterra series theory with high-order spectrum and KAC index to characterize the fault degree of analog circuits is proposed. The multi-pulse excitation method is used to identify the Volterra kernel function, and the higher-order spectrum and its slice method are used. The second-order and third-order kernel functions are visually characterized. Finally, the Kernel Assurance Criterion is introduced to quantitatively analyze the kernel function. The results show that the nonlinear analog circuit system which identified with this method can be used to characterize the system state accurately. The comparison of the faults in the Sallen-Key filter circuit shows that the high-order and its slice spectrum and KAC index can be used to extract nonlinear fault features, and which can use Volterra kernel function with qualitative analysis and quantitative representation, also can be extended to the comparison and analysis of soft faults in nonlinear analog circuits, and has certain practical significance for feature extraction of fault degree of nonlinear analog circuits.

References

- [1] Aminian, F., M. Aminian, and H.W. Collins, Jr., Analog fault diagnosis of actual circuits using neural networks. *IEEE Transactions on Instrumentation & Measurement*, 2002. 51 (3): p. 544-550.
- [2] Roh, J. and J.A. Abraham, Subband filtering for time and frequency analysis of mixed-signal circuit testing. *IEEE Transactions on Instrumentation & Measurement*, 2004. 53 (2): p. 602-611.
- [3] Tadeusiewicz, M., S. Halgas, and M. Korzybski, An algorithm for soft-fault diagnosis of linear

- and nonlinear circuits. *Circuits & Systems I Fundamental Theory & Applications IEEE Transactions on*, 2002. 49 (11): p. 1648-1653.
- [4] Sarathi Vasan, A.S., L. Bing, and M. Pecht, Diagnostics and Prognostics Method for Analog Electronic Circuits. *IEEE Transactions on Industrial Electronics*, 2013. 60 (11): p. 5277-5291.
- [5] Yang, C., et al., Fault Modeling on Complex Plane and Tolerance Handling Methods for Analog Circuits. *IEEE Transactions on Instrumentation & Measurement*, 2013. 62 (10): p. 2730-2738.
- [6] Hanhaitao, Mahongguang, et al., Fault Diagnosis Method of Analog Circuits Based on Characteristics of the Nonlinear Frequency Spectrum and KPCA. *TRANSACTIONS OF CHINA ELECTROTECHNICAL SOCIETY*, 2012. 27 (8): p. 248-254.
- [7] Hanhaitao, Mahongguang, et al., Fault diagnosis of nonlinear analog circuits based on sensitivity analysis and Volterra series. *JOURNAL OF CIRCUITS AND SYSTEMS*, 2013. 18 (1): p. 17-22.
- [8] Schetzen, M., The Volterra and Wiener theories of nonlinear systems. *Proceedings of the IEEE*, 2005. 70 (3): p. 316-317.
- [9] PENG Zhi Ke , CHENG Chang Ming. Volterra series theory: A state-of-the-art review [J]. *Chinese Science Bulletin*, 2015, (20): 1874-1888.
- [10] Li Hong-Wei, Zhou Yun-Long, et al., The sliced trispectrum fluctuation characteristics and flow pattern representation of the nitrogen-water two-phase flow of small channel. 2013 *Acta Phys. Sin.* Vol. 62, No. 14 (2013) 140505
- [11] CAI Qi-zhi, HUANG Yi-jian. Fault Diagnosis of the Speed Control Valve Using the Slices of Trispectrum. *Journal of Huaqiao University(Natural Science)*, 2009. 30(1): p. 16-21.
- [12] CHENG Changming. *Volterra Series Based Nonlinear System Identification And Its Application*. 2015. Shanghai Jiao Tong University